LXXV Международная конференция «ЯДРО-2025. Физика атомного ядра и элементарных частиц. Ядерно-физические технологии»

«Excitation of isomeric states of Hg and Au isotopes in photonuclear reactions»

S.S. Belyshev[1,2], A.A. Kuznetsov[1,2], O.V. Poriadina[1], N. Yu. Fursova[1,2], V. V. Khankin[2]

[1]Lomonosov Moscow State University, Department of Physics

[2]Skobeltsyn Institute of Nuclear Physics

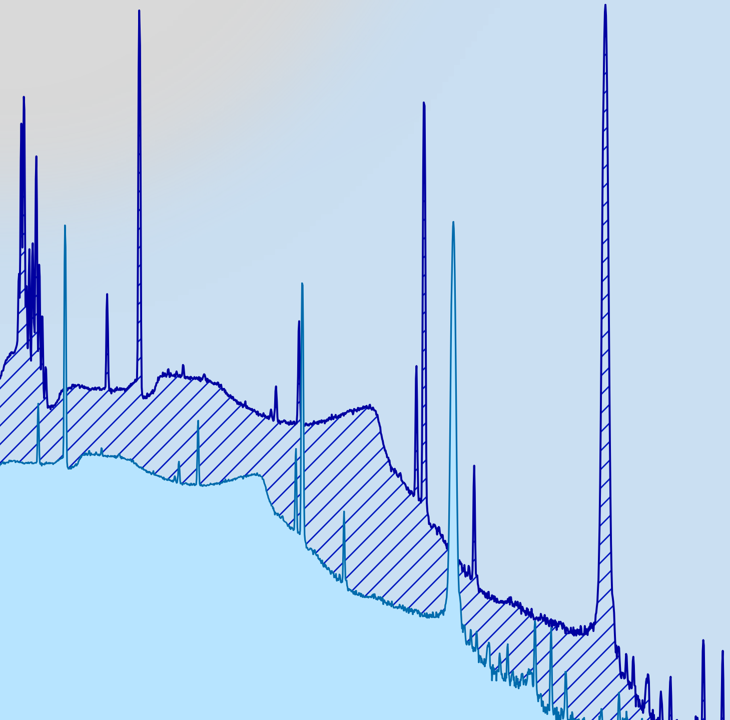

Saint Petersburg - 2025

The irradiation method of **a natural mixture of Hg isotopes** sample with bremsstrahlung radiation with E^m = 55 MeV

Converter target thickness: 0.2 mm
Irradiation time: 670 seconds
Thickness of the irradiated target: 2.8 mm

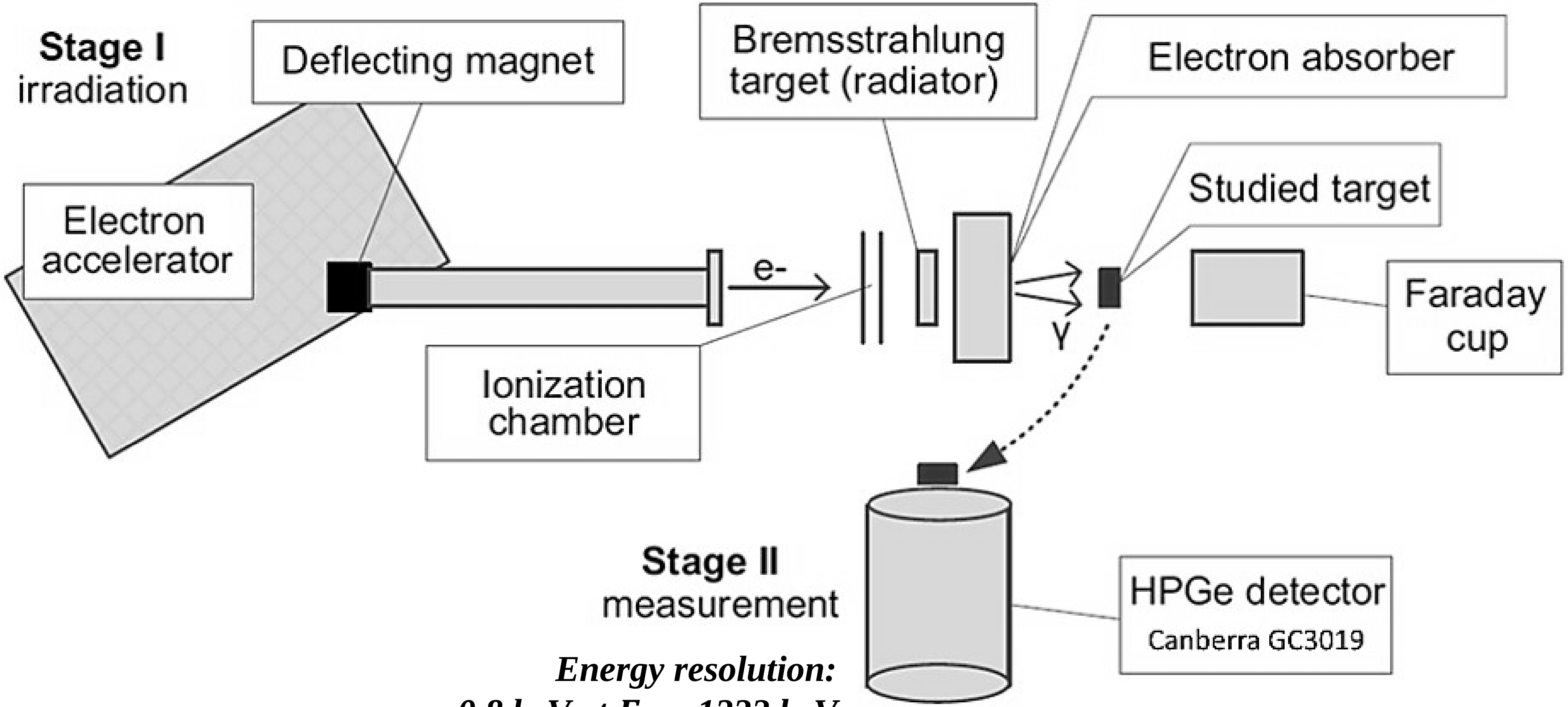

Energy resolution:
0.8 keV at E_γ = 1332 keV

The yields of photonuclear reactions were determined from **the peaks of the γ-lines** in **the spectra of the residual activity** of the irradiated mercury sample

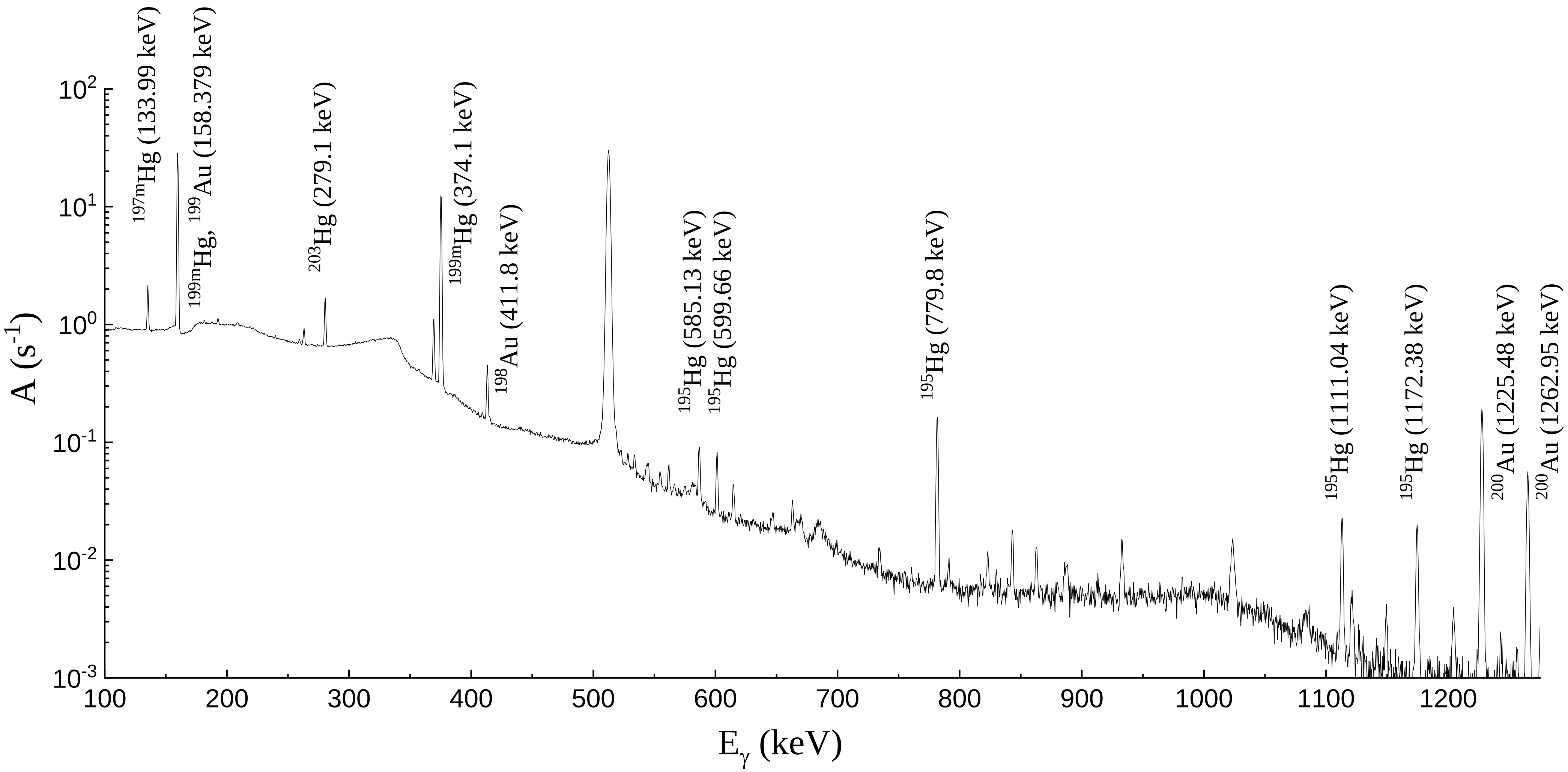

The spectrum of residual activity of the irradiated Hg sample (data set was carried out for 4 hours)

Determination of the yields of **single-channel** and **two-channel** photonuclear reactions

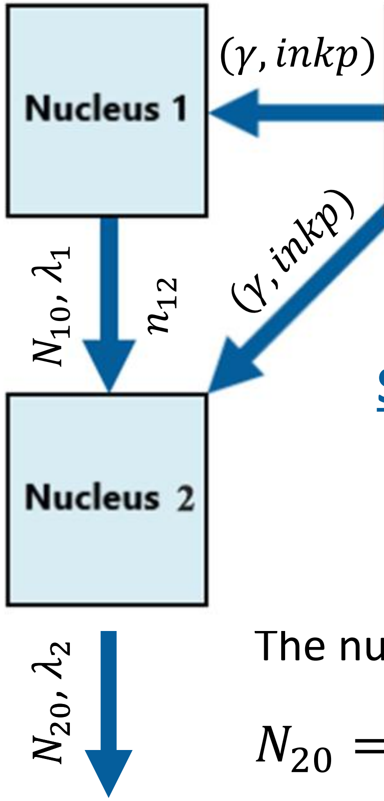

The number of nuclei at the end of irradiation: $N_{10} = \dfrac{S}{kI_\gamma\left(e^{-\lambda_1(t_2-t_1)} - e^{-\lambda_1(t_3-t_1)}\right)}$

I_γ – intensity of the γ-line
k – detector efficiency
S – the peak area in the spectrum of residual activity during the measurement
I – accelerator current

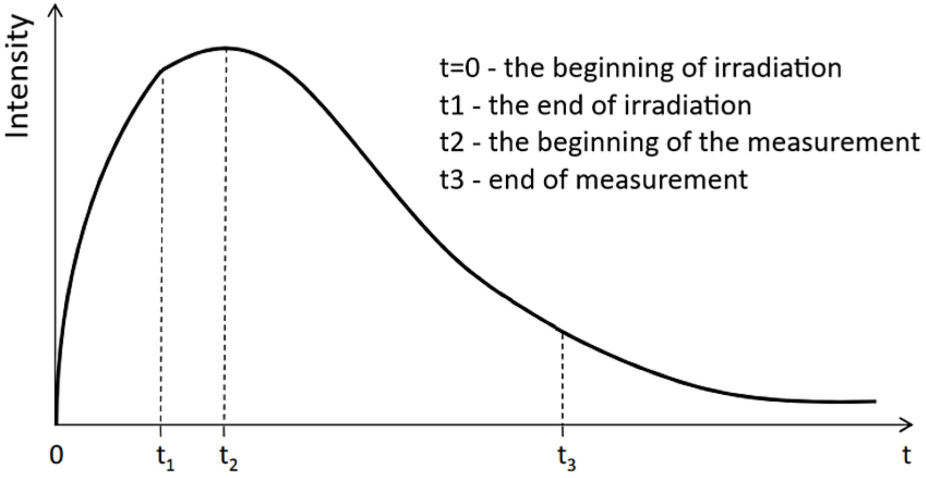

Single-channel reaction yield:

$$\boxed{Y_1^{exp} = \frac{N_{10}\lambda_1}{I(1 - e^{-\lambda_1 t_1})}}$$

The number of nuclei at the end of irradiation:

$$N_{20} = \frac{\lambda_1 n_{12} N_{10}}{\lambda_2 - \lambda_1} + \frac{S}{kI_\gamma\left(e^{-\lambda_2(t_2-t_1)} - e^{-\lambda_2(t_3-t_1)}\right)} - \frac{\lambda_2 n_{12} N_{10}}{\lambda_2 - \lambda_1}\left(\frac{e^{-\lambda_1(t_2-t_1)} - e^{-\lambda_1(t_3-t_1)}}{e^{-\lambda_2(t_2-t_1)} - e^{-\lambda_2(t_3-t_1)}}\right),$$

Two-channel reaction yield:

$$\boxed{Y_2^{exp} = \frac{\lambda_2}{I(1 - e^{-\lambda_2 t_1})} N_{20} - n_{12} Y_1 \left(\frac{\lambda_2\left(1 - e^{-\lambda_1 t_1}\right) - \lambda_1\left(1 - e^{-\lambda_2 t_1}\right)}{(\lambda_2 - \lambda_1)(1 - e^{-\lambda_2 t_1})}\right)}$$

, where n_{12} – the decay coefficient

Based on the obtained **yields, the isomeric ratios IR** of photonuclear reactions were calculated for the studied isotopes of **^{195,197}Hg and ^{198,200}Au at $E^m = 55$ MeV**

$$\mathbf{IR = Y_h/Y_l} \quad \text{or} \quad \mathrm{IR} = \sigma_h/\sigma_l,$$

where Y_h, Y_l and σ_h, σ_l – yields and cross sections of the formation of high-spin and low-spin states, respectively

The isomerism of atomic nuclei is caused by a **large difference in the spins** or **deformations of the isomeric state relative to the ground state.**

The population probability of isomers in photonuclear reactions **depends on:**

1. The reaction energy
2. The orbital angular momentum of emitted particles (which depends on their energy and the shell structure of the excited nucleus)
3. The spin-parity characteristics of the final state
4. Probabilities of cascading transitions from higher-lying states

Based on the obtained **yields, the isomeric ratios IR** of photonuclear reactions were calculated for the studied isotopes of **^{195,197}Hg and ^{198,200}Au at $E^m = 55$ MeV**

$$\mathbf{IR = Y_h/Y_l} \quad \text{or} \quad \mathrm{IR} = \sigma_h/\sigma_l,$$

where Y_h, Y_l and σ_h, σ_l – yields and cross sections of the formation of high-spin and low-spin states, respectively

Isotope	*The main reaction of isotope production*	J_m^P	J_g^P	IR_{exp}	IR_{TALYS} *(actual bremsstrahlung spectrum)*
^{195}Hg	$^{196}\mathrm{Hg}(0^+)(\gamma,1n)^{195m,g}\mathrm{Hg}$	13/2$^+$	1/2$^-$	0.481 ± 0.016	0.345
^{197}Hg	$^{198}\mathrm{Hg}(0^+)(\gamma,1n)^{197m,g}\mathrm{Hg}$	13/2$^+$	1/2$^-$	0.147 ± 0.009	0.094
^{198}Au	$^{199}\mathrm{Hg}(1/2^-)(\gamma,1p)^{198m,g}\mathrm{Au}$ $^{200}\mathrm{Hg}(0^+)(\gamma,1n1p)^{198m,g}\mathrm{Au}$	12$^-$	2$^-$	0.0026 ± 0.0006	0.0576
^{200}Au	$^{201}\mathrm{Hg}(3/2^-)(\gamma,1p)^{200m,g}\mathrm{Au}$ $^{202}\mathrm{Hg}(0^+)(\gamma,1n1p)^{200m,g}\mathrm{Au}$	12$^-$	1$^-$	0.0019 ± 0.0003	0.0671

The **experimental** isomeric ratios for **^{195}Hg, ^{197}Hg are compared** with **theoretical** calculations according to the **TALYS** program, as well as with works found in the literature

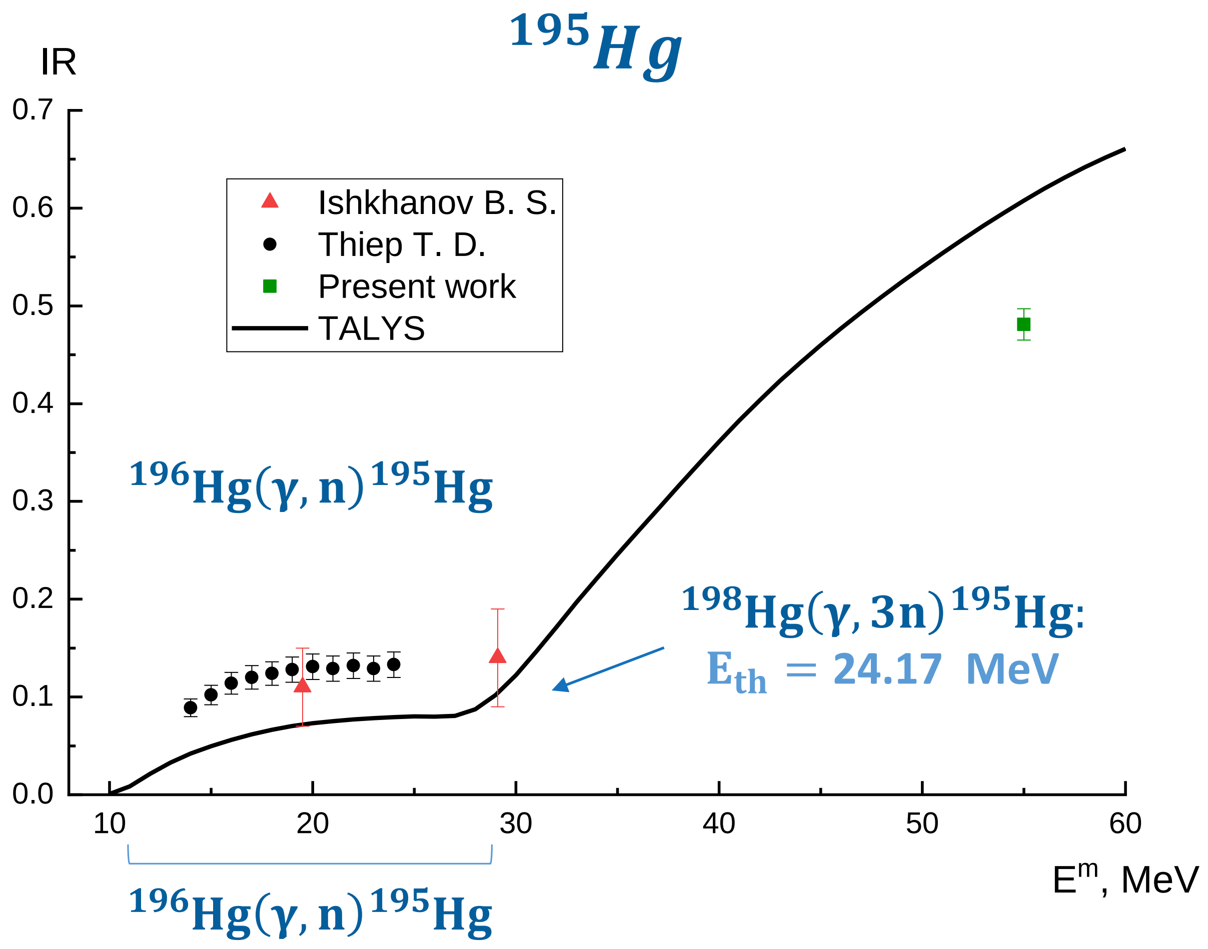

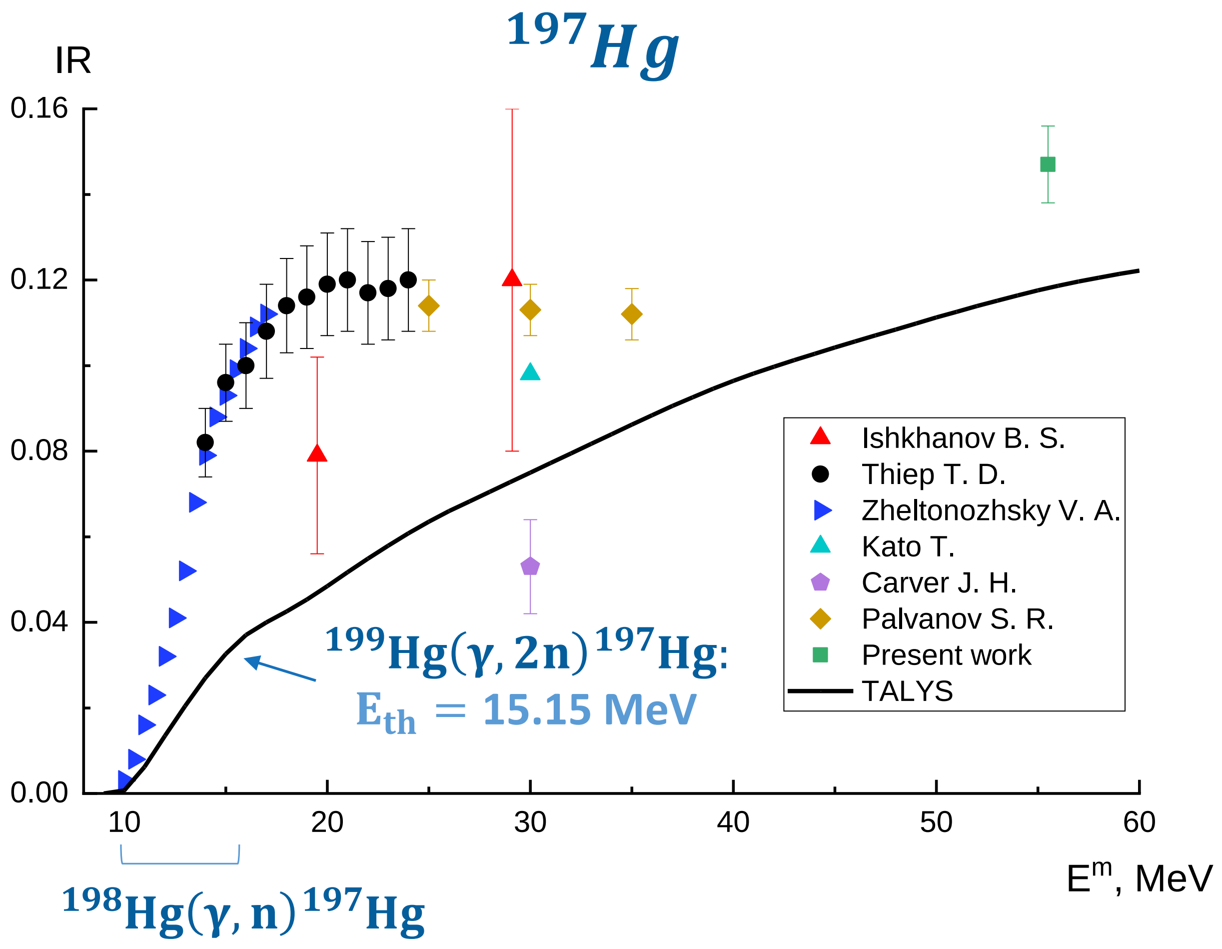

The dependence of the isomeric ratios of IR (^{195}Hg) (left graph) and IR (^{197}Hg) (right) on the irradiation energy

There is a clear **decrease in partial yields as the absolute spin difference increases.** Based on **experimental** data, **quadratic-exponential approximation curve $Y/Y_{tot} = exp(-A\Delta I^2 - B\Delta I)$ was fitted**

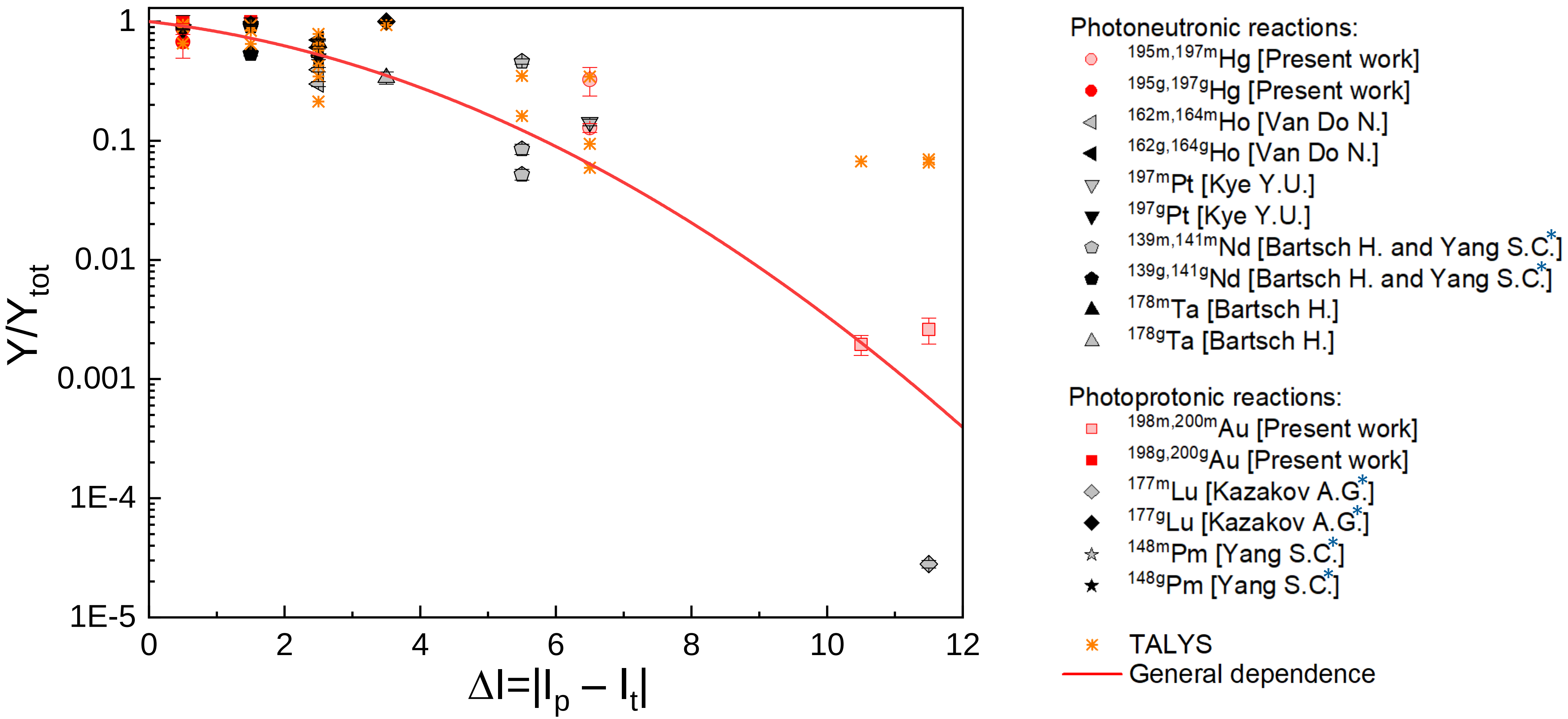

*The dependence of partial yields of high-spin (lightly shaded points) and low-spin (fully shaded points) states **at an electron energy of 55 MeV** on the absolute value of the spin difference between the product and target $\Delta I = |I_p - I_t|$*

*Targets of natural isotopic composition were used, and multi-nucleon reactions were taken into account

Based on **experimental** data, **linear-exponential approximation curve $Y/Y_{tot} = exp(-A\Delta I)$ was fitted. The parameter $|I_p(I_p+1) - I_t(I_t+1)|$ shows better correlation** with the population probabilities of metastable and ground states

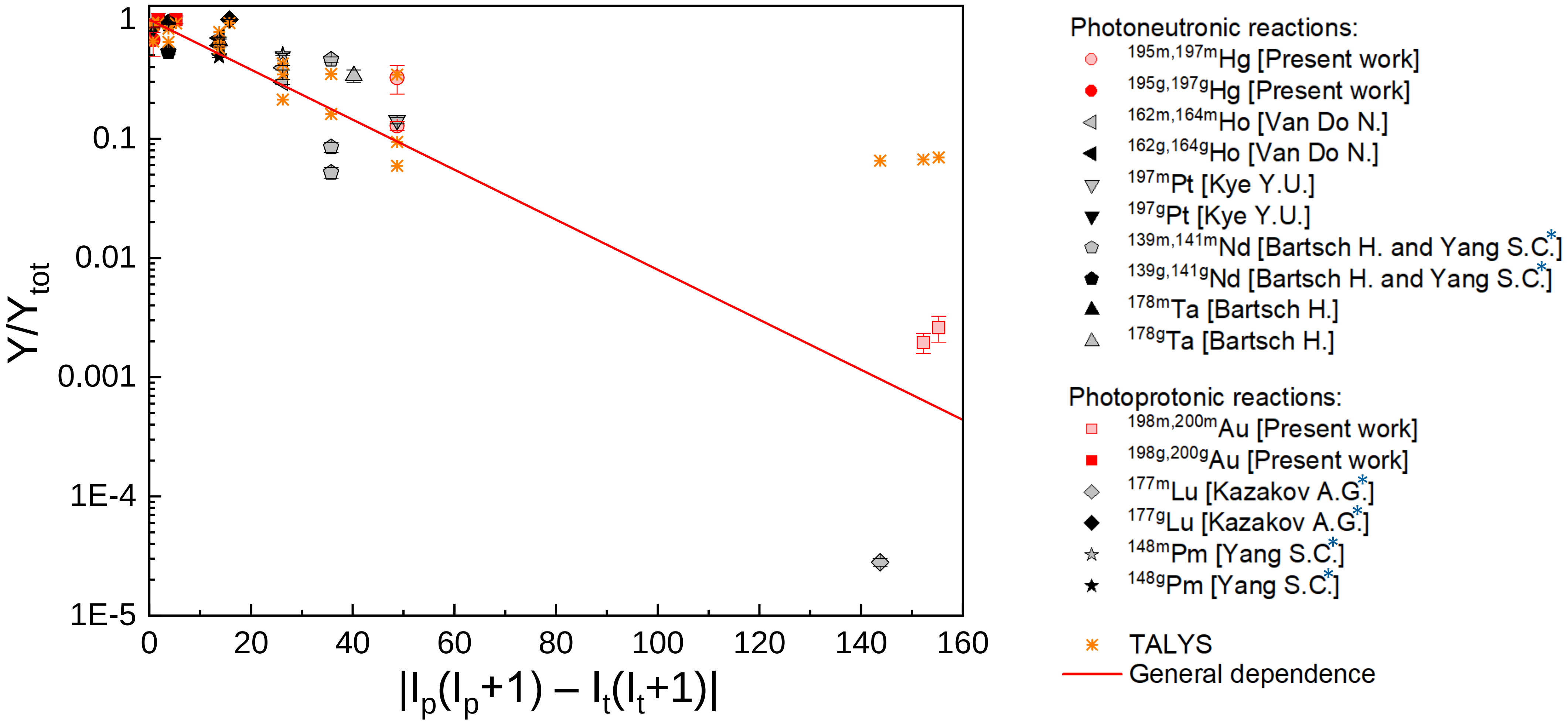

*The dependence of partial yields of high-spin (lightly shaded points) and low-spin (fully shaded points) states **at an electron energy of 55 MeV** on the absolute value $\Delta I = |I_p(I_p+1) - I_t(I_t+1)|$*

Karamian S.A. Phys. Atom. Nuclei **76**, 1437-1443 (2013).

Under identical conditions, **the isomeric ratio $IR = Y_h/Y_l$ is consistently higher for photoproton reactions than for photoneutron reactions due to the Coulomb barrier effect**

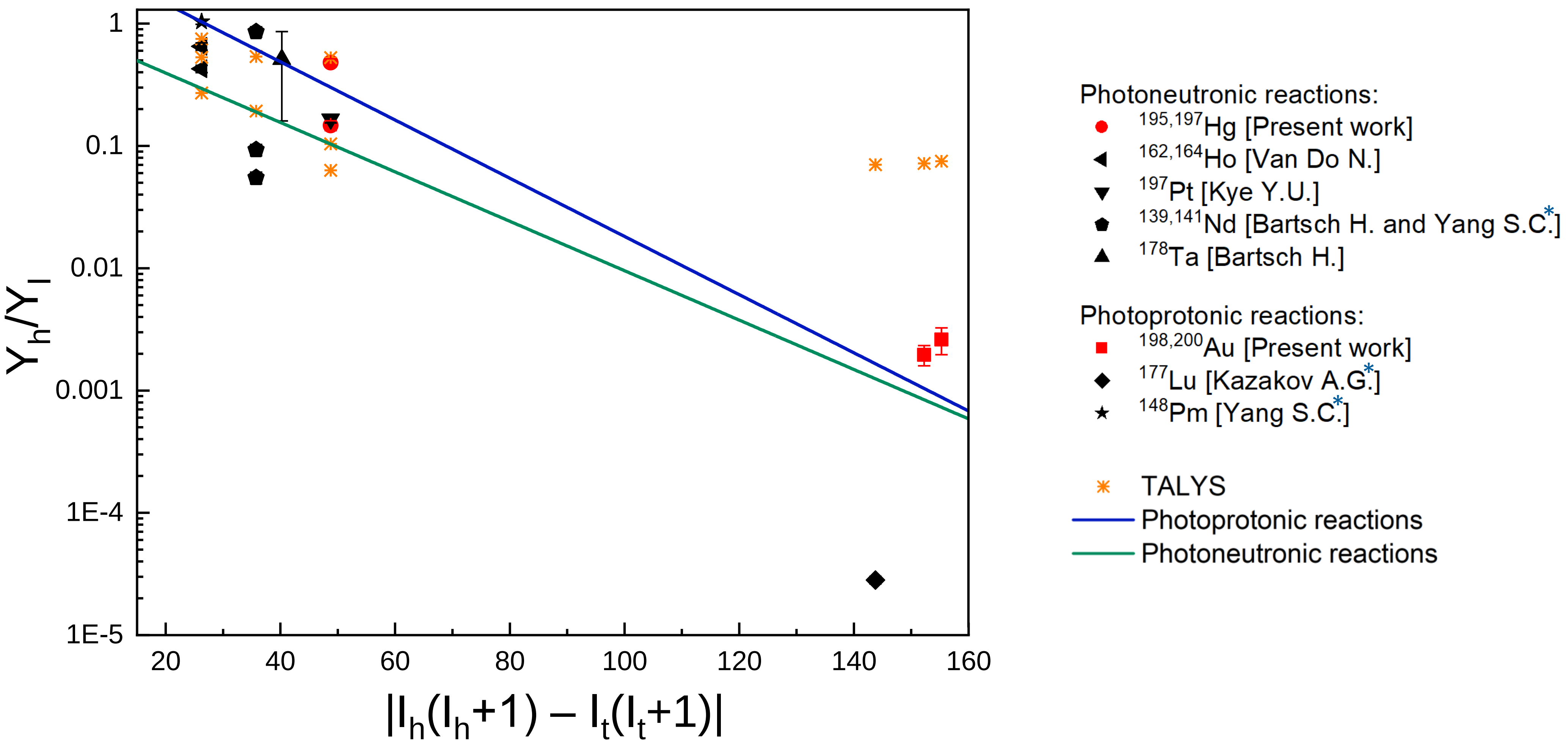

The dependence of isomeric ratios ***at an electron energy of 55 MeV*** *on the absolute value of the spin difference between the high-spin state and target* $\Delta I = |I_h(I_h+1) - I_t(I_t+1)|$

Karamian S.A. Phys. Atom. Nuclei **76**, 1437-1443 (2013).

A **final** conclusion on the existence of dependence common to all heavy nuclei **can be made only after additional studies of single-channel reactions either on enriched targets or at lower irradiation energies**

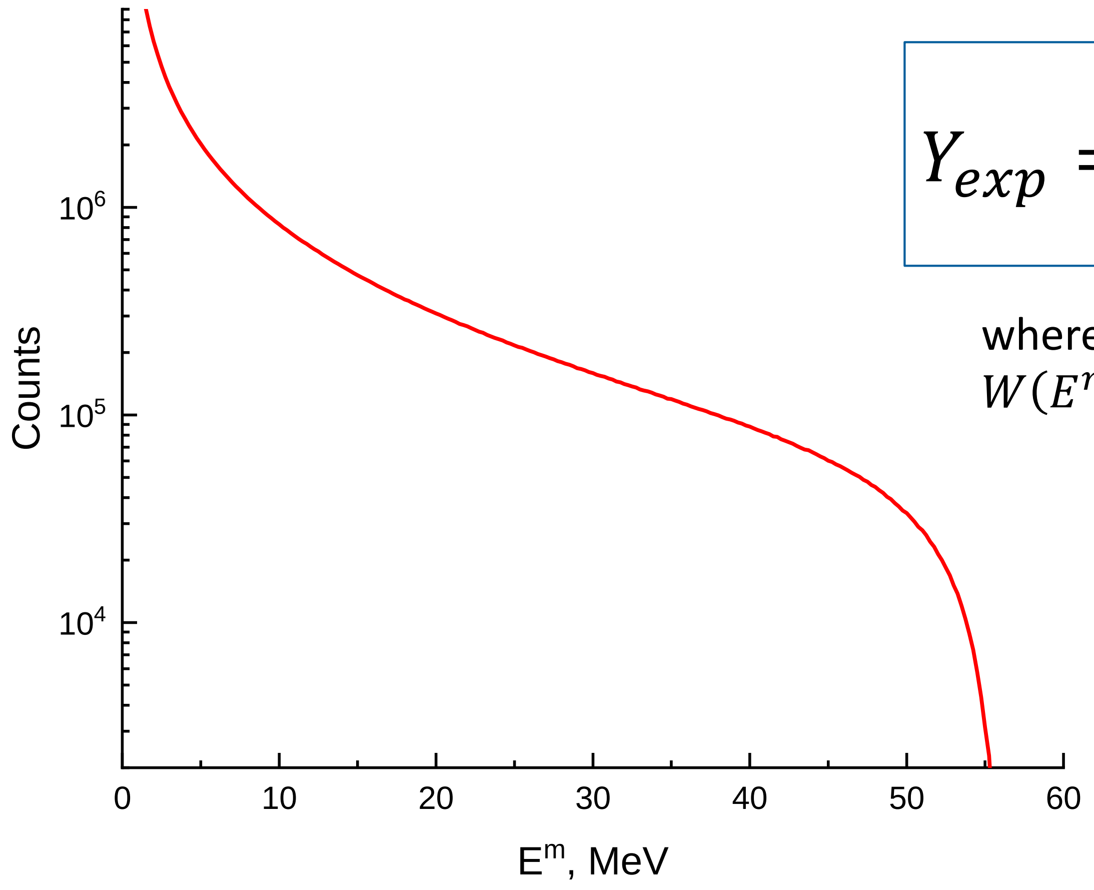

Bremsstrahlung spectrum with an upper endpoint energy of $E^m = 55\ MeV$

$$Y_{exp} = k_{norm} M \int_{E_{th}}^{E^m} W(E^m, E)\sigma(E)dE\,,$$

where M - the surface concentration of the target nuclei
$W(E^m, E)$ - bremsstrahlung γ-ray spectrum

$\Rightarrow$ **To reconstruct the reaction cross section $\boldsymbol{\sigma(E)}$**, one must solve **a complex unfolding inverse problem** (employing the Penfold-Leiss approaches, Cook's least-structure method, Tikhonov regularization, among others).

The use of **monochromatic γ-ray beams** overcomes fundamental limitations of conventional sources and **enables direct measurements of nuclear reaction cross-sections**. **The NCPhM CRS** (Compton radiation source) represents such a facility

$$R = I_\gamma \cdot M \cdot d \cdot \sigma(E_\gamma),$$

where $I_\gamma \sim 5 \cdot 10^8\ s^{-1}$ – the intensity of gamma quanta, $M = \frac{\rho}{M_r} \cdot N_A$ – the surface concentration of the target nuclei, M_r – the molecular weight of the target, $d = 1\ cm$ – the target thickness, $\sigma(E_\gamma)$ – the reaction cross-section at E_γ (calculated with TALYS)

Parameters		*Reaction*			
		$^{165}Ho(\gamma,3n)^{162m}Ho$	$^{165}Ho(\gamma,3n)^{162g}Ho$	$^{165}Ho(\gamma,1n)^{164m}Ho$	$^{165}Ho(\gamma,1n)^{164g}Ho$
E_{th}, MeV		23.18	23.07	8.13	7.99
$\sigma(E_\gamma), mbar$ $(TALYS)$	$E_\gamma = 10$ MeV	0	0	$\cong$ 13.462	$\cong$ 51.327
	$E_\gamma = 20$ MeV	0	0	$\cong$ 1.769	$\cong$ 5.861
	$E_\gamma = 30$ MeV	$\cong$ 8.107	$\cong$ 11.512	$\cong$ 0.276	$\cong$ 0.920
R, s^{-1}	$E_\gamma = 10$ MeV	0	0	$\sim$ 216100	$\sim$ 824100
	$E_\gamma = 20$ MeV	0	0	$\sim$ 28400	$\sim$ 94100
	$E_\gamma = 30$ MeV	$\sim$ 130200	$\sim$ 184800	$\sim$ 4400	$\sim$ 14800

Grigorenko L.V. et al. Fizmat **1** (2024).

The total number of detected events from the NCPhM CRS was evaluated, demonstrating the feasibility of the proposed measurement methodology

Parameters		***Reaction***			
		$^{165}Ho(\gamma,3n)^{162m}Ho$	$^{165}Ho(\gamma,3n)^{162g}Ho$	$^{165}Ho(\gamma,1n)^{164m}Ho$	$^{165}Ho(\gamma,1n)^{164g}Ho$
$E_\gamma, keV\ (I_\gamma, \%)$		282.86 (11.3%)	1319.3 (3.8%)	56.64 (6.5%)	91.40 (2.2%)
Detector efficiency *k (5 cm)*		0.012	0.006	0.0007	0.0014
$T_{1/2}$		67.1 min	15.0 min	36.6 min	28.8 min
N_{det} $(t = T_{1/2})$	$E_\gamma = 10\ MeV$	0	0	~ 5	~ 13
	$E_\gamma = 20\ MeV$	0	0	~ 0.6	~ 1.4
	$E_\gamma = 30\ MeV$	~ 88	~ 21	~ 0.10	~ 0.23
Background N_f		~ 16	~ 0.4	~ 15	~ 14

Grigorenko L.V. et al. Fizmat **1** (2024).

Threshold and spin factors strongly influence the yields of the photonuclear reactions

1. **Experimental isomeric yield ratios** for $^{195,197}\mathrm{Hg}$ and $^{198,200}\mathrm{Au}$ **at E^m = 55 MeV** were calculated. Comparing the obtained IR with **the TALYS program** calculations indicates **acceptable agreement** for **photoneutron** reactions and **poor agreement** for **photoproton** reactions.
2. Possible **reasons for the discrepancies** between experimental and theoretical values include **theoretical parameters** and the use of the **bremsstrahlung spectrum** calculated **based on the Seltzer-Berger tables instead of the actual** bremsstrahlung spectrum in thick targets.
3. The **theoretical** isomeric ratios calculated using the TALYS program reach **saturation.**
4. For many **heavy-nuclei** targets, **a systematic dependence of the yield on the spin factor has been observed.**
5. **The isomeric ratio** for **photoproton** reactions **is** systematically **higher** than for **photoneutron** reactions due to the presence of the **Coulomb barrier.**
6. The conducted evaluations demonstrate a fundamentally new capability to perform activation experiments and study isomeric states using the developed **the NCPhM CRS.**

Isomeric ratios IR were obtained for **heavy**-nuclei isotopes produced in **photonuclear** reactions at the maximum electron accelerator energy of $E_m = 55$ **MeV**

Main reaction	J_m^P	J_g^P	$IR_{exp} = Y_m/Y_g$	*Reference*
$^{196}Hg(0^+)\ (\gamma,1n)^{195m,g}Hg$	$13/2^+$	$1/2^-$	0.481 ± 0.016	Present work*
$^{198}Hg(0^+)\ (\gamma,1n)^{197m,g}Hg$	$13/2^+$	$1/2^-$	0.147 ± 0.009	Present work*
$^{199}Hg(3/2^-)\ (\gamma,1p)^{198m,g}Au$ $^{200}Hg(0^+)\ (\gamma,1n1p)^{198m,g}Au$	12^-	2^-	0.0026 ± 0.0006	Present work*
$^{201}Hg(3/2^-)(\gamma,1p)^{200m,g}Au$ $^{202}Hg(0^+)(\gamma,1n1p)^{200m,g}Au$	12^-	1^-	0.0019 ± 0.0003	Present work*
$^{178}Hf(0^+)(\gamma,1p)^{177m,g}Lu$	$23/2^-$	$7/2^+$	$(28.2 \pm 2.0) \cdot 10^{-6}$	[A.G. Kazakov]*
$^{165}Ho(7/2^-)(\gamma,1n)^{164m,g}Ho$	6^-	1^+	0.427 ± 0.029	[N. Van Do]
$^{165}Ho(7/2^-)(\gamma,3n)^{162m,g}Ho$	6^-	1^+	0.652 ± 0.045	[N. Van Do]
$^{198}Pt(0^+)(\gamma,1n)^{197m,g}Pt$	$13/2^+$	$1/2^-$	0.166 ± 0.012	[Y.U. Kye]
$^{149}Sm(7/2^-)(\gamma,1p)^{148m,g}Pm$ $^{150}Sm(0^+)(\gamma,1n1p)^{148m,g}Pm$	$5^-, 6^-$	1^-	1.035 ± 0.048	[S.C. Yang]*
$^{142}Nd(0^+)(\gamma,1n)^{141m,g}Nd$	$11/2^-$	$3/2^+$	0.055 ± 0.006	[H. Bartsch]
$^{181}Ta(7/2^+)(\gamma,3n)^{178m,g}Ta$	1^+	7^-	1.96 ± 0.35	[H. Bartsch]
$^{142}Nd(0^+)(\gamma,1n)^{141m,g}Nd$ $^{143}Nd(7/2^-)(\gamma,2n)^{141m,g}Nd$	$11/2^-$	$3/2^+$	0.093 ± 0.010	[S.C. Yang]*
$^{142}Nd(0^+)(\gamma,3n)^{139m,g}Nd$ $^{143}Nd(7/2^-)(\gamma,4n)^{139m,g}Nd$	$11/2^-$	$3/2^+$	0.859 ± 0.081	[S.C. Yang]*

*Targets of natural isotopic composition were used, and multi-nucleon reactions were taken into account

An interesting feature: **the isomeric ratio for ^{195}Hg decreases sharply** in the region of electron energies around 24 MeV, followed by an increase

$$IR_{nat} = \frac{\sum_i \eta_i \sigma_{h_i}}{\sum_i \eta_i \sigma_{l_i}},$$

where σ_h, σ_l – cross sections of high-spin and low-spin state formation, η_i – abundance of the isotope in the natural mixture

^{195}Hg

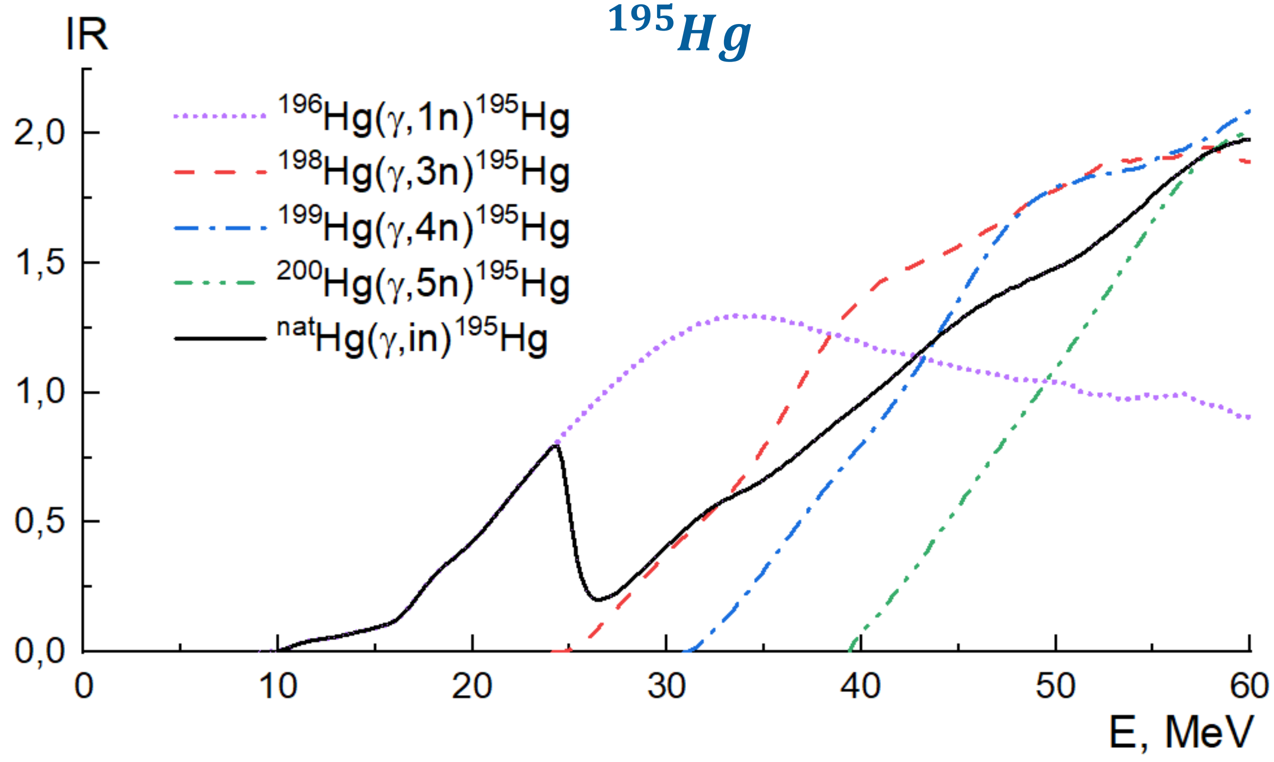

^{197}Hg

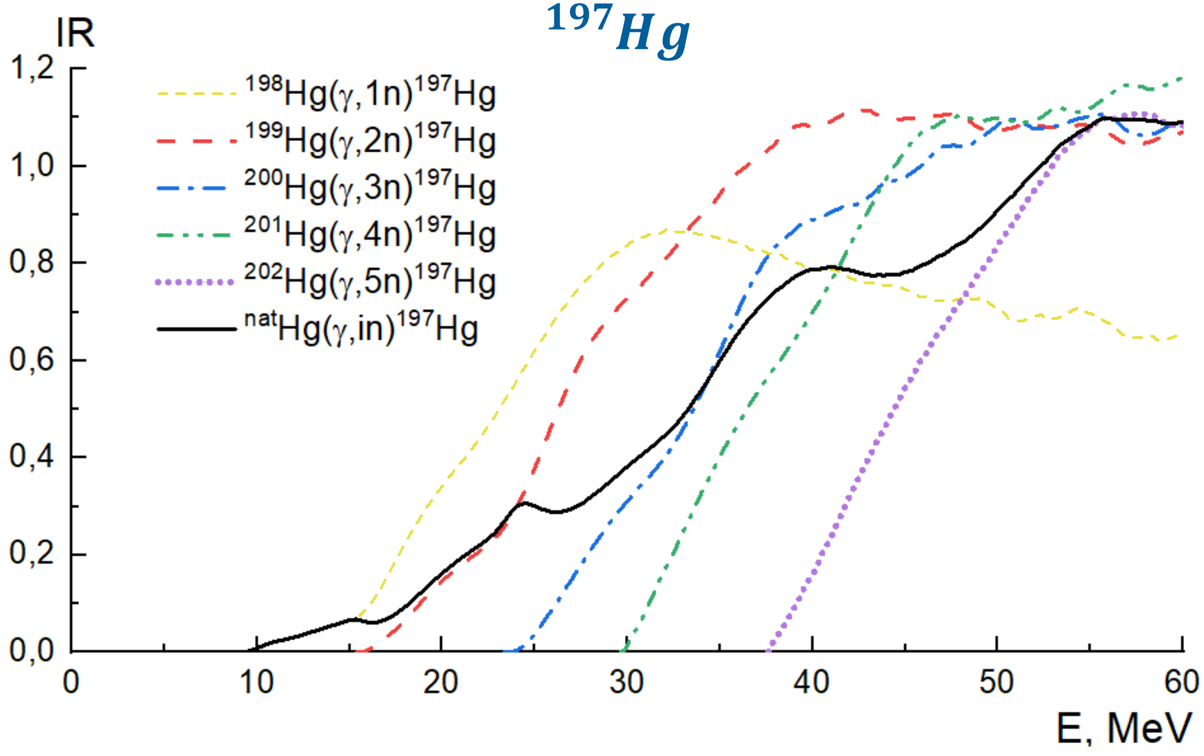

The dependence of the isomeric-to-ground state formation cross section ratio for ^{195}Hg (left graph) and ^{197}Hg (right graph) on the γ-quanta energy, calculated using the TALYS program

Radioisotopes ^{198}**Au и** ^{199}**Au** are a promising **theranostic pair**

^{199}Au:

The average energy of the emitted β-particle is 84 keV ($\lambda \approx 100$ mm), which gives this radionuclide the ability to deliver energy, for example, to micrometastases and tumor cells near the surface of organs. Thus, it is well suited for radioimmunotherapy.

^{198}Au:

It is used in radiotherapy of various types of cancer. In recent years, it has been used as gold nanoparticles for the development of radiopharmaceuticals.

Nanostructures labeled ^{198}Au or ^{199}Au are also being investigated as a way to visualize oncological diseases in vivo.

Various decay channels were identified by **the energy of the peaks E_γ in the spectrum** and **the half-lives $T_{1/2}$** of the isotopes formed

Isotope	*$T_{1/2}$*	*Isotope production reaction*	*E_γ, keV (I_γ, %)*
^{195g}Hg	10.53 h	$^{nat}\mathrm{Hg}(\gamma,in) = 0.00155 \cdot {}^{196}\mathrm{Hg}(\gamma,1n) + 0.0997 \cdot {}^{198}\mathrm{Hg}(\gamma,3n) + 0.1687 \cdot {}^{199}\mathrm{Hg}(\gamma,4n) + 0.2310 \cdot {}^{200}\mathrm{Hg}(\gamma,5n)$	180.11 (1.9), 207.1 (1.57), 261.75 (1.5), 585.13 (1.99), 599.66 (1.78), 779.8 (7.0), 1111.04 (1.44), 1172.38 (1.24)
^{195m}Hg	41.6 h	$^{nat}\mathrm{Hg}(\gamma,in) = 0.00155 \cdot {}^{196}\mathrm{Hg}(\gamma,1n) + 0.0997 \cdot {}^{198}\mathrm{Hg}(\gamma,3n) + 0.1687 \cdot {}^{199}\mathrm{Hg}(\gamma,4n) + 0.2310 \cdot {}^{200}\mathrm{Hg}(\gamma,5n)$	261.75 (30.9), 387.87 (2.15), 560.27 (7.0)
^{197g}Hg	64.14 h	$^{nat}\mathrm{Hg}(\gamma,in) = 0.0997 \cdot {}^{198}\mathrm{Hg}(\gamma,1n) + 0.1687 \cdot {}^{199}\mathrm{Hg}(\gamma,2n) + 0.2310 \cdot {}^{200}\mathrm{Hg}(\gamma,3n) + 0.1318 \cdot {}^{201}\mathrm{Hg}(\gamma,4n) + 0.2986 \cdot {}^{202}\mathrm{Hg}(\gamma,5n)$	77.351 (18.7), 191.437 (0.632), 268.78 (0.04)
^{197m}Hg	23.8 h	$^{nat}\mathrm{Hg}(\gamma.in) = 0.0997 \cdot {}^{198}\mathrm{Hg}(\gamma,1n) + 0.1687 \cdot {}^{199}\mathrm{Hg}(\gamma,2n) + 0.2310 \cdot {}^{200}\mathrm{Hg}(\gamma,3n) + 0.1318 \cdot {}^{201}\mathrm{Hg}(\gamma,4n) + 0.2986 \cdot {}^{202}\mathrm{Hg}(\gamma,5n)$	133.99 (33.0), 164.97 (0.26), 279.197 (6.0)
^{199m}Hg	42.6 m	$^{nat}\mathrm{Hg}(\gamma,in) = 0.2310 \cdot {}^{200}\mathrm{Hg}(\gamma,1n) + 0.1318 \cdot {}^{201}\mathrm{Hg}(\gamma,2n) + 0.2986 \cdot {}^{202}\mathrm{Hg}(\gamma,3n)$	158.3795 (52.0), 374.1 (13.8)
^{203}Hg	46.612 d	$0{,}0687 \cdot {}^{204}\mathrm{Hg}(\gamma,1n)$	279.1967 (81.0)

Various decay channels were identified by **the energy of the peaks E_γ in the spectrum** and **the half-lives $T_{1/2}$** of the isotopes formed

Isotope	*$T_{1/2}$*	*Isotope production reaction*	*E_γ, keV (I_γ, %)*
^{194}Au	38.02 h	$^{nat}\mathrm{Hg}(\gamma, \mathrm{in1p}) = 0{,}00155 \cdot {}^{196}\mathrm{Hg}(\gamma, 1\mathrm{n}1\mathrm{p}) + 0{,}0997 \cdot {}^{198}\mathrm{Hg}(\gamma, 3\mathrm{n}1\mathrm{p}) + 0{,}1687 \cdot {}^{199}\mathrm{Hg}(\gamma, 4\mathrm{n}1\mathrm{p})$	328.455 (61.0)
^{196}Au	6.183 d	$^{nat}\mathrm{Hg}(\gamma, \mathrm{in1p}) = 0.0997 \cdot {}^{198}\mathrm{Hg}(\gamma, 1\mathrm{n}1\mathrm{p}) + 0.1687 \cdot {}^{199}\mathrm{Hg}(\gamma, 2\mathrm{n}1\mathrm{p}) + 0.2310 \cdot {}^{200}\mathrm{Hg}(\gamma, 3\mathrm{n}1\mathrm{p})$	332.983 (22.9), 355.684 (87.0)
^{198g}Au	2.695 d	$^{nat}\mathrm{Hg}(\gamma, \mathrm{in1p}) = 0.1687 \cdot {}^{199}\mathrm{Hg}(\gamma, 1\mathrm{p}) + 0.2310 \cdot {}^{200}\mathrm{Hg}(\gamma, 1\mathrm{n}1\mathrm{p}) + 0.1318 \cdot {}^{201}\mathrm{Hg}(\gamma, 2\mathrm{n}1\mathrm{p})$	411.802 (96.0)
^{198m}Au	2.27 d	$^{nat}\mathrm{Hg}(\gamma, \mathrm{in1p}) = 0.1687 \cdot {}^{199}\mathrm{Hg}(\gamma, 1\mathrm{p}) + 0.2310 \cdot {}^{200}\mathrm{Hg}(\gamma, 1\mathrm{n}1\mathrm{p}) + 0.1318 \cdot {}^{201}\mathrm{Hg}(\gamma, 2\mathrm{n}1\mathrm{p})$	214.841 (77.0)
^{199}Au	3.139 d	$^{nat}\mathrm{Hg}(\gamma, \mathrm{in1p}) = 0.2310 \cdot {}^{200}\mathrm{Hg}(\gamma, 1\mathrm{p}) + 0.1318 \cdot {}^{201}\mathrm{Hg}(\gamma, 1\mathrm{n}1\mathrm{p}) + 0.2986 \cdot {}^{202}\mathrm{Hg}(\gamma, 2\mathrm{n}1\mathrm{p})$	158.3795 (40.0), 208.206 (8.73)
^{200g}Au	48.4 m	$^{nat}\mathrm{Hg}(\gamma, \mathrm{in1p}) = 0.1318 \cdot {}^{201}\mathrm{Hg}(\gamma, 1\mathrm{p}) + 0.2986 \cdot {}^{202}\mathrm{Hg}(\gamma, 1\mathrm{n}1\mathrm{p})$	367.943 (19.0), 1225.479 (10.7), 1262.950 (3.12)
^{200m}Au	18.7 h	$^{nat}\mathrm{Hg}(\gamma, \mathrm{in1p}) = 0.1318 \cdot {}^{201}\mathrm{Hg}(\gamma, 1\mathrm{p}) + 0.2986 \cdot {}^{202}\mathrm{Hg}(\gamma, 1\mathrm{n}1\mathrm{p})$	255.87 (71.0), 367.943 (73.0)

The yields of photonuclear reactions were determined from **the peaks of the γ-lines** in **the spectra of the residual activity** of the irradiated mercury sample

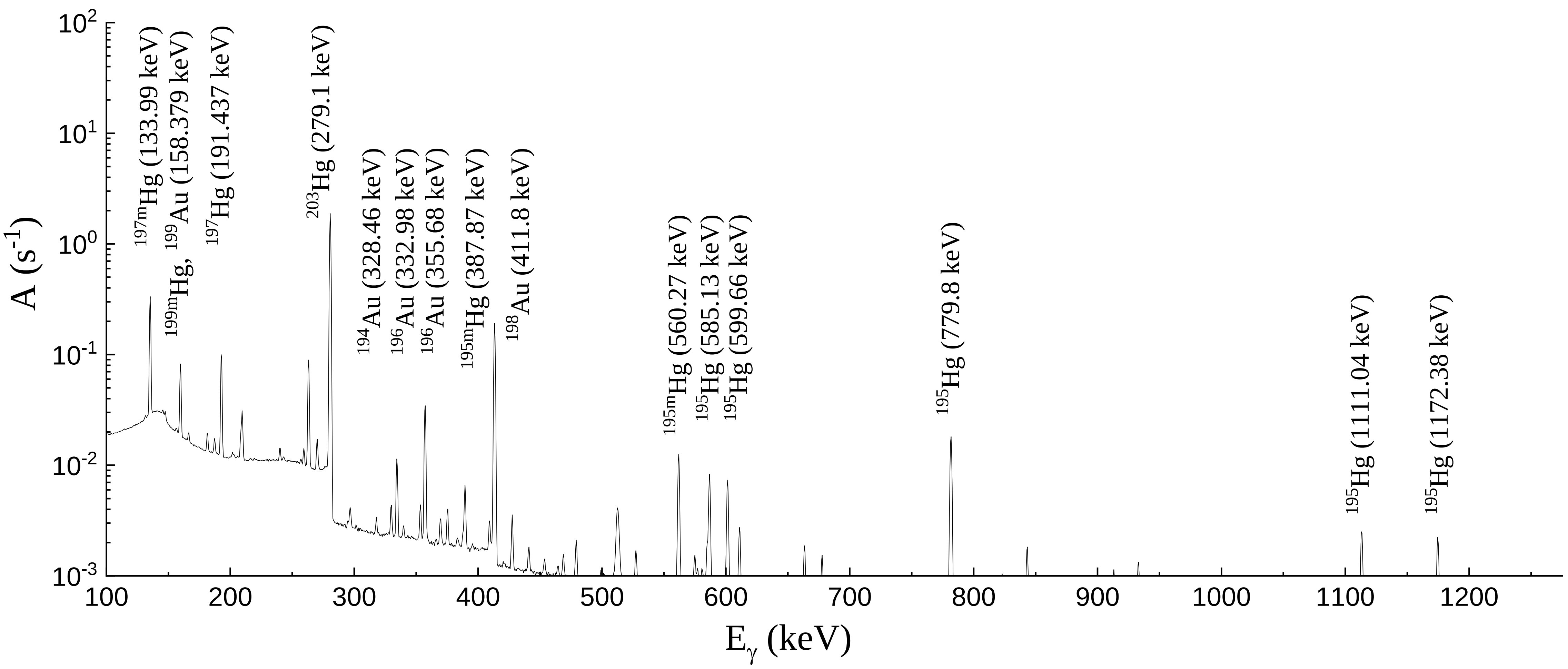

The spectrum of residual activity of the irradiated Hg sample (data set was carried out for 16 days)

The sources of the peaks were identified using **The Lund/LBNL Nuclear Data database** and **the determination of the half-life $T_{1/2}$**

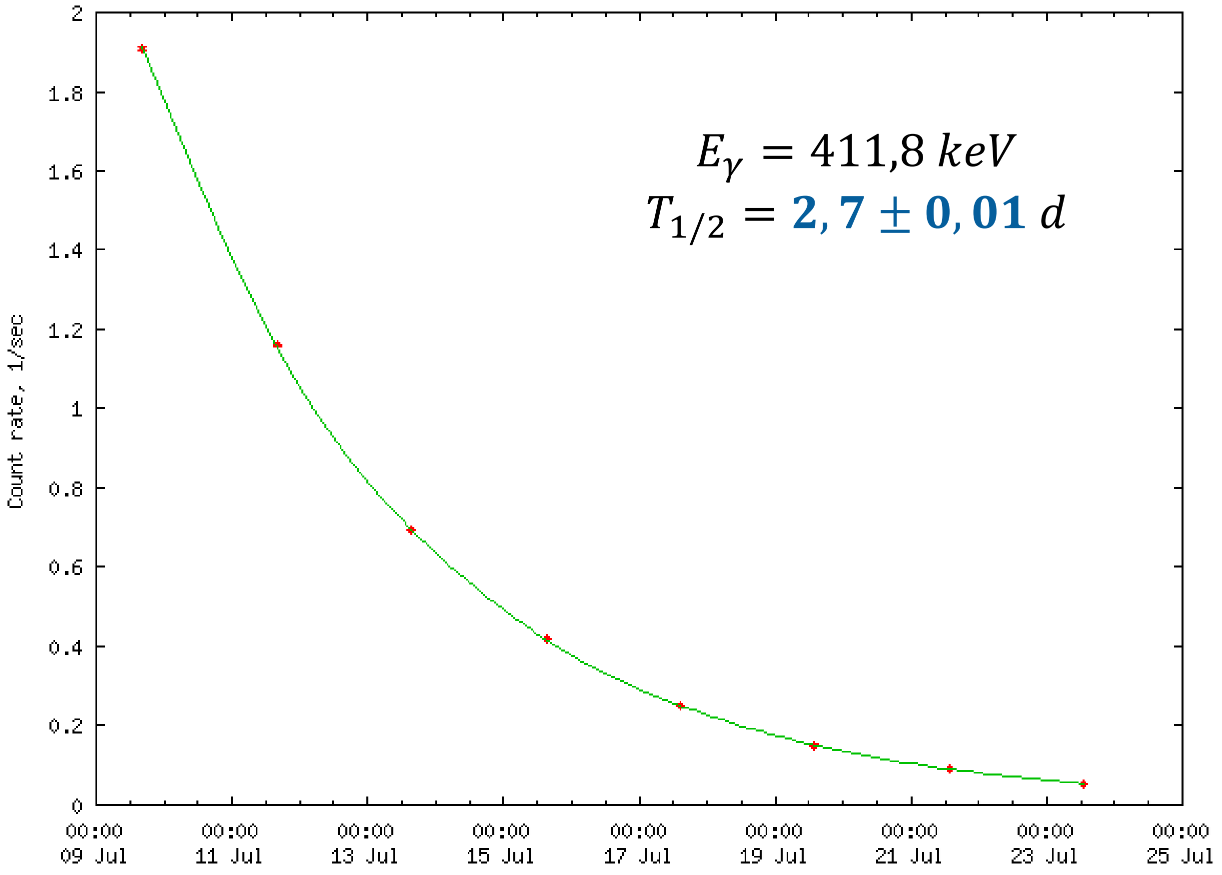

The half-life determined by approximating a decrease in the peak area corresponding to an energy of 411.8 keV

$T_{1/2}$ were identified using an automatic acquisition system.

Gammas from ^{198}Au (2.69517 d *21*)

Eγ (keV)	Iγ (%)	Decay mode
411.80205 *17*	96	β⁻
675.8836 *7*	0.804 *3*	β⁻
1087.684 *3*	0.159 *2*	β⁻

Thus, the peak of 411.8 keV corresponds to the **pure** decay channel **^{198}Au**

A source*:* The Lund/LBNL Nuclear Data

The results of **theoretical** calculations of the cross sections of photonuclear reactions on Hg isotopes using **the combined photonucleon reaction model** (CMPR) were analyzed

Isotope	*Isotope production reaction*	*E_{th}, МэВ*	*Y (55 МэВ)$_{exp}$, e^{-1}*	*Y_{CMPR}, e^{-1}*	*Y_{TALYS}, e^{-1}*
$^{195g+m}\mathrm{Hg}$	$^{nat}\mathrm{Hg}(\gamma, in) =$ $0.0015 \cdot {}^{196}\mathrm{Hg}(\gamma, 1n)$ $+ 0.0997 \cdot {}^{198}\mathrm{Hg}(\gamma, 3n)$ $+ 0.1687 \cdot {}^{199}\mathrm{Hg}(\gamma, 4n)$	8.90 24.17 30.83	$(3.8 \pm 1.0) \cdot 10^{-6}$	$3.992 \cdot 10^{-6}$	$5.516 \cdot 10^{-6}$
$^{197g+m}\mathrm{Hg}$	$^{nat}\mathrm{Hg}(\gamma, in) =$ $0.0997 \cdot {}^{198}\mathrm{Hg}(\gamma, 1n)$ $+ 0.1687 \cdot {}^{199}\mathrm{Hg}(\gamma, 2n)$ $+ 0.2310 \cdot {}^{200}\mathrm{Hg}(\gamma, 3n)$	8.45 15.15 23.18	$(1.00 \pm 0.07) \cdot 10^{-4}$	$0.982 \cdot 10^{-4}$	$1.025 \cdot 10^{-4}$
$^{199m}\mathrm{Hg}$	$^{nat}\mathrm{Hg}(\gamma, in) =$ $0.2310 \cdot {}^{200}\mathrm{Hg}(\gamma, 1n)$ $+ 0.1318 \cdot {}^{201}\mathrm{Hg}(\gamma, 2n)$ $+ 0.2986 \cdot {}^{202}\mathrm{Hg}(\gamma, 3n)$	8.56 14.79 22.54	$(1.56 \pm 0.09) \cdot 10^{-5}$	-*	$8.417 \cdot 10^{-6}$
$^{203}\mathrm{Hg}$	$^{nat}\mathrm{Hg}(\gamma, in) =$ $0.0687 \cdot {}^{204}\mathrm{Hg}(\gamma, 1n)$	7.49	$(4.97 \pm 0.25) \cdot 10^{-5}$	$4.587 \cdot 10^{-5}$	$4.081 \cdot 10^{-5}$

* within the framework of the CMPR, the total cross section for the ground and metastable states is obtained

There is **a good agreement** of the experimental data within the error limits with the results of the calculation according to **the CMPR** in the case of **photoproton** reactions, according to **the TALYS program, discrepancies are observed**

Isotope	*Isotope production reaction*	E_{th}, МэВ	Y (55 МэВ)$_{exp}$, e^{-1}	Y_{CMPR}, e^{-1}	Y_{TALYS}, e^{-1}
^{194}Au	$^{nat}Hg(\gamma, in1p) =$ $0.0015 \cdot {}^{196}Hg(\gamma, 1n1p)$ $+ 0.0997 \cdot {}^{198}Hg(\gamma, 3n1p)$	14.93 30.24	$(1.74 \pm 0.11) \cdot 10^{-8}$	$8.530 \cdot 10^{-9}$	$9.781 \cdot 10^{-9}$
^{196}Au	$^{nat}Hg(\gamma, in1p) =$ $0.0997 \cdot {}^{198}Hg(\gamma, 1n1p)$ $+ 0.1687 \cdot {}^{199}Hg(\gamma, 2n1p)$	15.18 21.84	$(2.34 \pm 0.12) \cdot 10^{-7}$	$2.000 \cdot 10^{-7}$	$1.577 \cdot 10^{-7}$
$^{198g+m}Au$	$^{nat}Hg(\gamma, in1p) =$ $0.1687 \cdot {}^{199}Hg(\gamma, 1p)$ $+ 0.2310 \cdot {}^{200}Hg(\gamma, 1n1p)$	7.25 15.28	$(1.11 \pm 0.06) \cdot 10^{-6}$	$1.329 \cdot 10^{-6}$	$3.468 \cdot 10^{-7}$
^{199}Au	$^{nat}Hg(\gamma, in1p) =$ $0.2310 \cdot {}^{200}Hg(\gamma, 1p)$ $+ 0.1318 \cdot {}^{201}Hg(\gamma, 1n1p)$	7.70 13.93	$(1.34 \pm 0.07) \cdot 10^{-6}$	$1.384 \cdot 10^{-6}$	$3.382 \cdot 10^{-7}$
$^{200g+m}Au$	$^{nat}Hg(\gamma, in1p) =$ $0.1318 \cdot {}^{201}Hg(\gamma, 1p)$ $+ 0.2986 \cdot {}^{202}Hg(\gamma, 1n1p)$	7.68 15.44	$(9.2 \pm 0.8) \cdot 10^{-7}$	$8.864 \cdot 10^{-7}$	$2.757 \cdot 10^{-7}$